

1 **From Bright Windows to Dark Spots: Snow Cover Controls Melt Pond Optical**  
2 **Properties during Refreezing**

3

4 **P. Anhaus<sup>1\*</sup>, C. Katlein<sup>1</sup>, M. Nicolaus<sup>1</sup>, M. Hoppmann<sup>1</sup>, C. Haas<sup>1,2</sup>**

5

6 <sup>1</sup>Alfred-Wegener-Institut Helmholtz-Zentrum für Polar- und Meeresforschung, Bremerhaven,  
7 Germany

8 <sup>2</sup>Department of Environmental Physics, University of Bremen, Bremen, Germany

9

10 \*Corresponding author: Philipp Anhaus ([philipp.anhaus@awi.de](mailto:philipp.anhaus@awi.de))

11

12 **Key Points:**

- 13 • Refrozen melt ponds may collect a thicker snow cover compared to bare sea ice due to their  
14 recessed topography
- 15 • Such snow-covered melt ponds transmit less light compared to bare ice of similar type
- 16 • This scenario has not been documented before and should be accounted for in studies  
17 involving light in a refreezing Arctic Ocean

18

19 **Word count = 4232**

20

21 **Abstract**

22 Melt ponds have a strong impact on the Arctic surface energy balance and the ice-associated  
23 ecosystem because they transmit more solar radiation compared to bare ice. In the existing  
24 literature, melt ponds are considered as bright windows to the ocean, even during freeze-up in  
25 autumn. In the central Arctic during the summer-autumn transition in 2018, we encountered a  
26 situation where more snow accumulated on refrozen melt ponds compared to the adjacent bare ice,  
27 leading to a reduction in light transmittance of the ponds even below that of bare ice. Supporting  
28 results from a radiative transfer model suggest that melt ponds with a snow cover  $>0.04$  m lead to  
29 lower light transmittance than adjacent bare ice. This scenario has not been described in the  
30 literature before, but has potentially strong implications for example on autumn ecosystem activity,  
31 oceanic heat budget and thermodynamic ice growth.

32

33

34 **Plain Language Summary**

35 Arctic sea ice is covered with snow during autumn, winter and spring. During summer, melt ponds  
36 evolve in response to surface melting. After snow fall starts again in autumn, these ponds can be  
37 filled with a lot of snow compared to bare ice because of their recessed surface. Indeed, during an  
38 expedition close to the North Pole in summer and autumn 2018, we measured a thick snow cover  
39 on ponds. This thick snow cover reduced the light availability underneath the ponds to levels below  
40 that underneath adjacent bare ice. This is a surprising finding, because it is different from the  
41 established theory of high light availability underneath melt ponds during both summer and  
42 autumn and how this is described in most computer models. It has consequences for our

43 understanding of the ice-associated ecosystem (organisms that live in and under sea ice). It might  
44 also impact the mass and energy balance of central Arctic sea ice during summer-autumn transition  
45 when new sea ice starts forming.

46

## 47 **1 Introduction**

48 Snow controls the optical properties and, thus, regulates the energy as well as the mass balance of  
49 sea ice because of its high reflectivity (Grenfell and Maykut, 1977) and insulation (e.g., Sturm et  
50 al., 1997). The snow cover of Arctic sea ice is highly variable in time and space (Webster et al.,  
51 2018). The rougher the sea ice topography the more snow accumulates (Sturm et al., 2002; Massom  
52 et al., 1997), for example at the lee sides of pressure ridges (Webster et al., 2018), at windward  
53 sides of snow dunes (Dadic et al., 2013) and within the depression of melt ponds (Perovich et al.,  
54 2003). In turn, the distribution of snow, especially snow dunes, influence melt pond formation  
55 (Petrich et al., 2012a; Polashenski et al., 2012). Melt ponds also play a key role for the surface  
56 energy budget (Nicolaus et al., 2012) and the mass balance of sea ice (Flocco et al., 2015), as well  
57 as for the ice- and ocean-associated ecosystem (Arrigo, 2014). In general, in August-September  
58 the melt pond coverage peaks (Perovich et al., 2002) and open and mature ponds evolve towards  
59 refrozen and snow-covered ponds (Perovich et al., 2009). The areal fraction of melt ponds on  
60 Arctic first-year ice is up to 53% and 20-38% on multi-year ice (e.g., Webster et al., 2015; Nicolaus  
61 et al., 2012; Perovich et al., 2003; Fetterer and Untersteiner, 1998). This fraction has been shown  
62 to increase from 15% to 35% for multi-year ice based on observations (Perovich et al., 2009) and  
63 from 11% to 34% for the entire Arctic based on model simulations (Schröder et al., 2014). The  
64 amount of radiation that is reflected back to the atmosphere is significantly reduced for melt ponds  
65 compared to bare ice (e.g., Nicolaus et al., 2012). Instead, a considerable amount of radiation is

66 absorbed by and transmitted through melt ponds (e.g., Katlein et al., 2015; Nicolaus et al., 2012;  
67 Ehn et al., 2011; Light et al., 2008; 2015). Consequently, the ice underlying the melt ponds warms  
68 and can thin faster than bare ice during snow-free summer (Flocco et al., 2015; Hanson, 1965;  
69 Untersteiner, 1961).

70 The translucent melt ponds are often considered as bright windows in Arctic sea ice, even during  
71 autumn when their surface refreezes. The formation and occurrence of under-ice phytoplankton  
72 blooms are highly dependent on snow and sea ice conditions and, thus, on the under-ice light field  
73 (Ardyna et al., 2020). An Arctic-wide increase in the occurrence of the blooms was partly  
74 explained by the increasing fraction of melt ponds (Horvat et al., 2017). Lee et al. (2015) showed  
75 that ice algal masses accumulate in and under refrozen and snow-free melt ponds that favor higher  
76 light availability. They argue that algal accumulations in autumn can provide an important food  
77 source for higher trophic animals before and during winter.

78 This study documents a situation where a thicker snow cover accumulates on melt ponds compared  
79 to bare ice after snow fall starts in autumn. The thicker snow cover reduces the light availability  
80 under melt ponds to levels lower than under adjacent bare ice. Using data collected in the central  
81 Arctic close to the geographic North Pole during the transition from summer to autumn in 2018,  
82 we investigate the effect of snow accumulated on the refrozen melt ponds on the under-ice light  
83 availability. We compare two datasets that represent the summer and autumn conditions, which  
84 mainly consist of snow depth and ice thickness measurements, along with aerial images and under-  
85 ice transmittance data from a remotely operated vehicle (ROV). We apply a radiative transfer  
86 model to calculate an estimate for the snow accumulation threshold necessary for the light level to  
87 be lower under melt ponds compared to bare ice.

88

## 89 **2 Materials and Methods**

### 90 **2.1 Study Site**

91 The data presented in this study were collected during the Arctic Ocean 2018 MOCCHA – ACAS  
92 – ICE campaign (short: AO18) onboard the Swedish icebreaker *Oden*. During this campaign, a  
93 temporary ice camp was set up on drifting, ponded multi-year ice close to the geographic North  
94 Pole between 14 August and 14 September 2018. Snow depth, total sea ice thickness (ice thickness  
95 plus snow depth) and transmitted irradiance were measured in an area of approximately 100 m x  
96 100 m (Figure 1). Marker poles (M0 to M23) were deployed under the ice to facilitate ROV  
97 navigation and to obtain a better co-location of the data. The mean ice thickness of bare ice was  
98 1.9 m and of the ice underlying the melt ponds 1.7 m (Table S2). Melt ponds were on average 0.3  
99 m deep. Here we focus on two main datasets: measurements performed between 17 and 24 August  
100 represented summer conditions which were characterized by open or only slightly refrozen melt  
101 ponds and no snow cover, whereas measurements performed between 13 and 14 September  
102 represented autumn conditions which were characterized by refrozen and snow-covered melt  
103 ponds.

104

### 105 **2.2 Snow Depth and Sea Ice Thickness**

106 Snow depth point measurements with a horizontal spacing of 1 to 3 m and an accuracy of 0.01 m  
107 were obtained on the (pristine) study area using a Magna Probe (Snow-Hydro, Fairbanks, AK,  
108 USA, Sturm and Holmgren, 2018). On snow-covered bare ice the Magna Probe likely penetrates  
109 into the underlying surface scattering layer (SSL) leading to an overestimate in snow depth. The  
110 GPS position of each measurement was recorded by an integrated GPS with an accuracy of 2.5 m  
111 (Sturm and Holmgren, 2018).

112 Total (sea ice plus snow) thickness was determined using a ground-based electromagnetic  
113 induction sounding device (GEM-2, Geophex Ltd, Raleigh, NC, USA, Hunkeler et al., 2015) using  
114 the in-phase signal at a frequency of 18.33 kHz. The GEM-2 was placed on a sledge and dragged  
115 across the study area in a grid pattern at the very end of the campaign. The accuracy of the total  
116 thickness measurements is  $\pm 0.1$  m (Hunkeler et al., 2015). Finally, ice thickness was calculated  
117 from total thickness by subtracting the (interpolated) snow depths. GPS positions of snow depth  
118 and ice thickness measurements were subsequently corrected for ice drift using GPS recorders  
119 placed at the acoustic transponder locations to enable co-location with the transmittance  
120 measurements.

121 In addition, in situ snow depth, ice thickness, draft, freeboard, and melt pond depth were measured  
122 in drill holes at the marker locations using a tape measure on 17 August.

123

### 124 **2.3 Under-Ice Transmittance**

125 Horizontal transects of under-ice spectral irradiance were measured by a RAMSES-ACC hyper-  
126 spectral radiometer (TriOS GmbH, Rastede, Germany). The radiometer was mounted on a M500  
127 ROV (Ocean Modules, Åtvidaberg, Sweden, Katlein et al., 2017). The ROV was lowered into the  
128 water through a 2 x 2 m hole in the ice covered by a tent next to the study area (Figure 1).

129 The light transmittance was calculated by wavelength-integrating the transmitted irradiance from  
130 350 to 920 nm and normalizing by the incident downwelling planar irradiance recorded by an  
131 upward-looking reference sensor at the surface. The data were filtered for ROV pitch, roll and  
132 depth, and noise was filtered from the spectra. Using the photosynthetically active radiation (400  
133 to 700 nm) did not lead to qualitatively different results and conclusions in this work, and is thus  
134 not further considered here.

135 For under-ice navigation, the ROV was equipped with an acoustic long baseline positioning system  
136 (Pinpoint 1500 Linkquest, San Diego, CA, USA). We manually post-processed the ROV position  
137 to remove distortions caused by calibration uncertainties.

138

## 139 **2.4 Aerial Images**

140 Oblique aerial images were obtained during a helicopter flight on 23 August (summer) and by a  
141 drone on 13 September (autumn). Those were used to retrieve the geographic coordinates of the  
142 melt ponds. The images were corrected for camera perspective and georeferenced using the marker  
143 locations measured by a terrestrial laser scanner (VZ-400i, RIEGL, Horn, Austria). Melt ponds in  
144 the image were detected using a simple threshold criterion. All pixels within the study area where  
145  $\text{mean}(R,G,B) < 70 + 0.5 \cdot B$  (Katlein et al., 2015) were classified as melt ponds, with R, G, B  
146 representing the integer values of the respective channels of the RGB color space (R=700 nm,  
147 G=525 nm, B=450 nm). We added a 2 m buffer by image dilation to account for horizontal light  
148 spreading (Ehn et al., 2011) and uncertainties of the ROV position.

149

## 150 **2.5 Radiative Transfer Model**

151 We modelled broadband reflection and under-ice transmittance using the radiative transfer model  
152 DORT2002 version 3.0 (Edström, 2005; Katlein et al., 2021). The model uses a discrete ordinate  
153 model geometry and is implemented in the MATLAB<sup>TM</sup> software. The ice geometry was  
154 approximated by three layers each for bare ice and melt ponds (Table S1): The bare ice consisted  
155 of the interior sea ice underlying a SSL with a freshly fallen snow layer of varying thickness on  
156 top. The melt ponds consisted of interior sea ice underlying the melt pond overlain by a snow layer  
157 of varying thickness. For simplicity, the situation without any snow will be referred to as “summer”

158 conditions whereas the snow covered scenario is referred to as “autumn” conditions. We used  
 159 typical inherent optical properties for multi-year ice (Katlein et al., 2021; Perron et al., 2021).

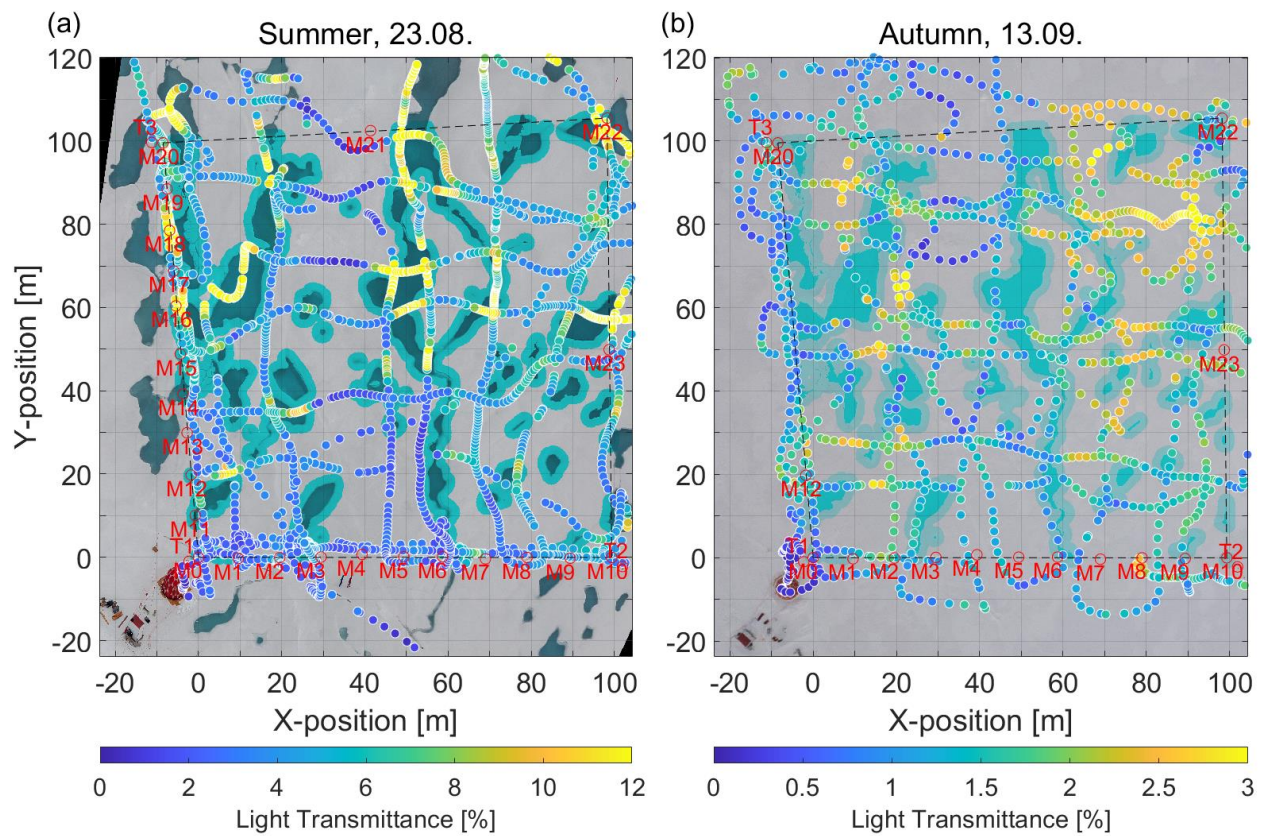
160

### 161 3 Results and Discussion

#### 162 3.1 Evolution of the Snow Cover in the Transition from Summer to Autumn

163 Figure 1 illustrates the distribution of melt ponds and bare ice and their surface properties during  
 164 the transition from summer to autumn in the study area.

165



166

167 **Figure 1:** Light transmittance through ponded sea ice during the transition from (a) summer to (b)  
 168 autumn. The data show ROV-based radiation measurements under (a) open melts ponds and (b)  
 169 refrozen and snow-covered ponds. The background images are orthorectified aerial images  
 170 acquired during (a) a low altitude helicopter flight and (b) a drone flight. Pixels within the study

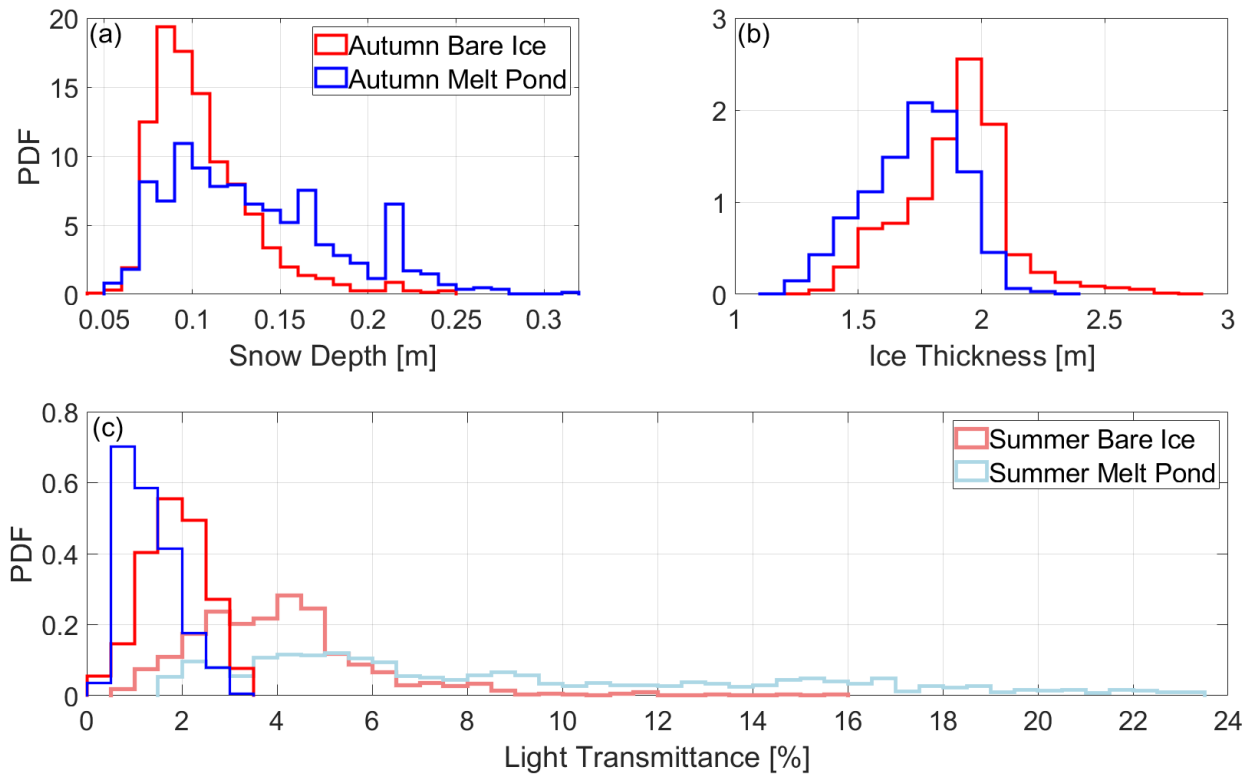
171 area that were classified as melt pond and used for further analysis are colored in blue. The melt  
172 ponds in (b) were refrozen and snow-covered but marked blue for illustration purposes. The edges  
173 around the melt ponds in (a) and (b) were dilated by a buffer of about 2 m. This area is indicated  
174 by a brighter blue. Red labels indicate the marker (M) and transponder locations (T). The ROV  
175 tent and control hut are visible on the lower left corners of the images. Note the different range in  
176 transmittance in (a) and (b).

177

178 On 23 August, the melt ponds were generally still open but in parts slightly refrozen at the surface  
179 (Figures 1a and S1). No significant snow fall occurred prior to 29 August (Vüllers et al., 2019),  
180 however a SSL of deteriorated ice with a mean thickness of 0.07 m was present. The passage of  
181 low-pressure systems between 29 August and 15 September brought precipitation accompanied  
182 by strong winds with speeds up to  $13 \text{ ms}^{-1}$  (Vüllers et al., 2019). This wind speed exceeded the  
183 threshold of  $8\text{-}10 \text{ ms}^{-1}$  under which divergence of large amounts of drifting snow is favourable  
184 (Van den Broeke and Bintanja, 1995). As a result, snow was deposited and re-distributed towards  
185 and caught by the recessed and refrozen melt ponds and their edges (Figure S1, Fetterer &  
186 Untersteiner, 1998; Perovich et al., 2003). This led to a higher mean snow accumulation on the  
187 ponds (0.14 m) compared to on bare ice (0.11 m) as measured on 13 September (Figure 2a, Table  
188 S2). On the melt ponds, higher snow depths were also much more frequently measured than on  
189 bare ice (modes of 0.17 and 0.22 m, Figure 2a).

190 The snow mostly covered the visible surface signature of the ponds (Figure 1). However, the ponds  
191 were still discernible because of their brighter appearance due to the higher snow depth compared  
192 to the adjacent bare ice (Figure 1b).

193



194

195 **Figure 2:** Histograms of measured (a) snow depth, (b) ice thickness, and (c) light transmittance of  
 196 melt ponds and bare ice.

197

198 The higher snow depth on the melt ponds can have important implications on the sea ice mass  
 199 balance related to the insulating effect of the snow cover (Sturm et al., 1997). Reduced heat loss  
 200 (Maykut, 1978) and thermodynamic ice growth (Merkouriadi et al., 2017; Maykut, 1978) as well  
 201 as delayed freeze-up of the liquid melt pond (Flocco et al., 2015) and induced bottom roughness  
 202 are expected.

203 The refrozen surface of the melt ponds alone reduces the heat release from the ocean through the  
 204 ice towards the atmosphere (Flocco et al., 2015). This hampers ice growth at both water-ice  
 205 interfaces of the refreezing pond, as well as between the sea ice bottom and the ocean in the  
 206 transition from autumn to winter. This can result in a delay of the complete freeze-up of the pond  
 207 by up to 60 days (Flocco et al., 2015). A thinner ice cover is more vulnerable to dynamic and

208 warming events. The presence of a snow cover on top of the refrozen pond surface and the still  
209 liquid melt pond underneath are expected to amplify those effects (Perovich et al., 2003). As a  
210 result of the reduced thermodynamic growth of the sea ice underlying melt ponds compared to  
211 bare ice, a generally rougher bottom topography might result, affecting the mass, momentum, heat,  
212 and salt fluxes at the sea ice-ocean interface.

213 The exact evolution of the thicker snow cover on melt ponds during refreezing depends on the  
214 sequence of weather events. Whether or not more snow accumulates on the refrozen melt ponds  
215 than on adjacent bare ice is governed by the wind speed and snow drift regime during and after the  
216 snow fall, by the snow properties, and by the roughness of the refrozen surface. Falling and  
217 deposited snow needs to be re-distributed before it can accumulate on the topographically recessed  
218 and rougher pond surface. Wet and heavy snow is more resistant to erosion by wind than low-  
219 density dry snow (e.g., Colbeck, 1979; Massom et al., 1997). For instance, new snow deposited on  
220 blue ice either by drifting or precipitation can hardly settle on the smooth and warm-temperate  
221 surface (Bintanja, 1999; Van den Broeke and Bintanja, 1995). In case downwind slopes are  
222 smooth, any snow that can temporarily accumulate is prevented from actually attaching to the  
223 surface (Dadic et al., 2013; Bintanja, 1999). On such surfaces, drifting snow is also prevented from  
224 becoming attached causing the wind to be stronger over the glazed surface than over the snow  
225 (Ferzzotti et al., 2002a). Furthermore, less snow will accumulate on smooth nilas with a low  
226 surface roughness (e.g., Sturm et al., 2002; Massom et al., 1997) than on surfaces with a higher  
227 surface roughness (e.g., Bintanja, 1999, Frezzotti, 2002b).

228

## 229 **3.2 Optical Properties**

230 The surface topography of the ponded ice cover was key in modulating spatial variability in snow  
231 depth and hence light transmittance: The presence of open melt ponds in summer and the  
232 variability in snow depth driven by the refrozen melt ponds in autumn also led to spatial and  
233 temporal variability in the under-ice light field. On 24 August, ROV-based mean and maximum  
234 transmittances of ponds (8.9% and 23.2%, respectively) were significantly higher than those of  
235 bare ice (4.1% and 15.5%, see also Figures 1a and 2c and Table S2). Histograms showed a bi-  
236 modal transmittance distribution of ponds and bare ice combined (Figure S2). The distribution also  
237 showed a characteristic long tail for ponds, indicating high spatial variability and different  
238 properties of the ponds. This distribution is typical for Arctic summer sea ice and results from the  
239 formation and development of the melt ponds (Katlein et al., 2015; 2019; Nicolaus et al., 2012;  
240 Schanke et al., 2021). The magnitudes of transmittance are similar to observations from Nicolaus  
241 et al. (2012) in the same region in August 2011. The maximum transmittance of the melt ponds  
242 also agrees to values found by Katlein et al. (2019).

243  
244 Due to the new snow cover on top of both the refrozen melt ponds and the bare ice (Figure 1b),  
245 the transmittance of both melt ponds and bare ice decreased (Figures 1 and S2, Table S2). The  
246 spatial variability in the transmittance of both melt ponds and bare ice was significantly reduced  
247 in autumn while the long tail of the high transmittances diminished, with very few observations  
248 higher than 3% (Figures 2c and S2, Table S2). In summer, approximately 80% (25%) of the  
249 transmittance measurements were higher than 3% (9%). Due to stronger and more frequent snow  
250 fall events that started to occur from 28 August (Vüllers et al., 2021), only 1% (0%) of the  
251 transmittances measurements in autumn were higher than 3% (9%).

252 Lee et al. (2011) describe observations indicating that melt ponds remain bright windows even in  
253 autumn after refreezing, although they did not consider a snow cover. This implies that the  
254 transmittance of melt ponds remains higher than that of bare ice. Katlein et al. (2019) showed that  
255 the bi-modal structure of transmittance during summer is conserved even during the first weeks of  
256 freeze-up in mid of September. They further suggest that the transmittances of both melt ponds  
257 and bare ice decrease gradually and equally in the transition from summer to autumn. Snow and  
258 particular re-distribution were present during their transmittance measurements, however those  
259 were not adequately considered.

260 We observed a different scenario than Lee et al. (2011) and Katlein et al. (2019). A thicker snow  
261 cover accumulated on melt ponds compared to adjacent bare ice because of the pond's recessed  
262 topography. This led to a lower mean transmittance of melt ponds (1.3%) than of bare ice (1.8%)  
263 in autumn (Figures 1 and 2c, Table S2). The transmittance distribution showed two distinct modes  
264 of 1.0% and 2.0% associated with melt ponds and bare ice, respectively (Figure 2c, Table S2).

265 Despite the reversal of the magnitude in the transmittance of melt ponds and bare ice, the spatial  
266 variability remained during autumn (Figure 1). This suggests that the spatial variability was still  
267 coupled to the ponds after snow accumulation and re-distribution and most likely also persisted  
268 into winter.

269 The transmittance of ridged ice with thicknesses up to 2.8 m was naturally still lower than that of  
270 the melt ponds (Figures S3b and 1b). Those measurements are included in the bare ice data and  
271 are represented in the tail of larger ice thicknesses in the histogram (Figure 2b).

272 This study provides first quantitative observations of lower light transmittance of melt ponds than  
273 of bare ice in autumn due to higher snow depths on the ponds. Major implications on the ice-

274 associated ecosystem and the energy balance of the sea ice might arise from those observations in  
275 case such a situation is viable for the entire Arctic which is very likely:

276 Lee et al. (2011) proposed that the soft refrozen surface of open melt ponds that are in connection  
277 with the ocean provides a fertile habitat for biomass in autumn. They pointed out that the biomass  
278 accumulated under the refrozen melt ponds serves as an important food source for higher trophic  
279 animals during the transition from autumn to winter and further into winter. However, as presented  
280 here, a snow cover significantly reduces the light availability in and under melt ponds in autumn,  
281 suggesting a limited suitability as habitat in terms of available light. Those observations lend  
282 support to a study by Lange et al. (2017), who found higher biomass values underneath hummocks  
283 on multi-year ice compared to adjacent level ice. Lange et al. (2017) attributed the differences in  
284 biomass accumulation to increased light availability under the hummocks resulting from a very  
285 thin or absent snow cover (Perovich et al., 2003). Our results and those of Lange et al. (2017)  
286 suggest that light conditions under sea ice in spring can already be initialized by melt pond  
287 coverage and snow distribution during autumn and may persist throughout winter.

288 Further, due to the common assumption that there is more light available under melt ponds than  
289 under bare ice also during autumn, processes and magnitudes of carbon uptake and biomass  
290 accumulation in models, might need to be adjusted with respect to our new observations.

291 Arndt and Nicolaus (2014) developed a parameterization to quantify the annual solar heat input  
292 through Arctic sea ice. For their calculations in autumn, they use for transmittances of melt ponds  
293 the fivefold (500%) of that of bare ice. However, our results showed that the modal transmittance  
294 of melt ponds is only half (50%) of that of bare ice once covered by the first snow (Table S2).  
295 Arndt and Nicolaus (2014) applied a constant summer mean melt pond fraction for multi-year ice  
296 of 29% (Rösel et al., 2012) and a transmittance of melt ponds for multi-year ice of 0.4%. They

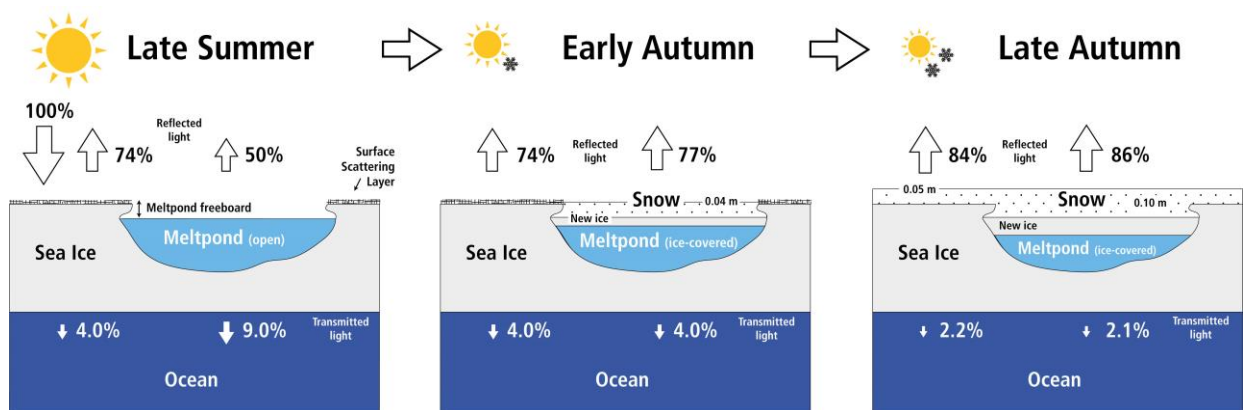
297 estimated the solar heat input into the ocean in September to  $0.69 \times 10^{19}$  J. We adopted their  
 298 parameters but used the ratio of transmittances between melt ponds and bare ice as presented in  
 299 the present study. As a result, the solar heat input into the ocean decreased by 61%. This shows,  
 300 that despite the generally low solar energy fluxes in autumn compared to in summer (e.g., Perovich  
 301 et al., 2011; Arndt and Nicolaus, 2014), our described effect could have an important impact on  
 302 the energy budget if valid in the entire Arctic. In this regard, our results might also impact the  
 303 heat stored in the upper ocean, the interior sea ice structure, as well as internal and basal melting.

304

### 305 **3.3 Radiative Transfer Model**

306 For the effect described above, it is of interest to quantify the threshold snow depth that is necessary  
 307 to decrease the transmittance of melt ponds below that of bare ice. In order to determine this  
 308 threshold depth, we used the radiative transfer model DORT2002. Figure 3 summaries the  
 309 observations of this study in a schematic which are supported by simulated albedo and  
 310 transmittance. For the situation without snow (summer), both the simulated transmittances of melt  
 311 ponds and bare ice (9% and 4%, respectively) were very similar to our observations (8.9% and  
 312 4.1%, respectively, Figures 3 and S4, Table S2).

313



314

315 **Figure 3:** Simulated reflected light (albedo) and transmitted light (transmittance) as a function of  
316 snow depth as modelled by DORT2002 for (left) snow-free melt ponds and bare ice, (middle)  
317 snow-covered melt ponds and snow-free bare ice, and (right) snow-covered melt ponds and bare  
318 ice. Properties used in the model are display in Table S1.

319

320 Incorporating an increasing snow cover from 0 to 0.20 m (autumn), our results yielded an  
321 exponential decrease in the transmittances of both melt ponds and bare ice (Figure S4). For a snow  
322 depth of approximately 0.04 m the transmittance of the melt ponds becomes equal to that of snow-  
323 free bare ice (Figures 3 and S4). This is in agreement with the observations presented earlier which  
324 showed that the transmittance of melt ponds was lower than that of bare ice for a 0.03 m higher  
325 mean snow depth on the ponds (Table S2). Figure 3c illustrates that the transmittance of melt ponds  
326 with a 0.10 m thick snow cover becomes lower than that of bare ice with a 0.05 m thick snow  
327 cover.

328 In our simulations, the influence of the thin ice lid on the melt ponds on the transmittance was  
329 neglected, as they were only partially existing, as for typical Arctic summer sea ice these are very  
330 translucent and scattering is small (Lu et al., 2018), indicated by their blue-green color (Figure 1a).

331

## 332 **5 Summary**

333 Snow depth measurements on a ponded sea ice floe in the transition from summer to autumn reveal  
334 that snow accumulation was on average 0.03 m higher on refrozen melt ponds than on adjacent  
335 bare ice favored by the ponds recessed surface. Using under-ice radiation measurements from a  
336 ROV we show that due to the thicker snow cover on the melt ponds the transmittance of the melt  
337 ponds can become lower than that of bare ice. Those results imply that melt ponds cannot be

338 universally considered as bright windows of Arctic autumn sea ice. Computations from a radiative  
339 transfer model indicate that a snow cover with a depth  $>0.04$  m accumulated on melt ponds result  
340 in transmittances of melt ponds becoming lower than that of snow-free bare ice. Our findings can  
341 have consequences for the autumn ecosystem activity, oceanic heat budget and thermodynamic  
342 ice growth if they can be observed in the entire Arctic.

343

### 344 **Acknowledgments**

345 This work was financed through the research programs PACES II and POF4 of the Alfred-  
346 Wegener-Institut Helmholtz-Zentrum für Polar- und Meeresforschung (AWI) and the Swedish  
347 Polar Research Secretariat (SPRS, grant no. AO18). Additional funding was received through the  
348 Diatom-ARCTIC project (NE/R012849/1; 03F0810A) as part of the Changing Arctic Ocean  
349 program (CAO), jointly funded by the UKRI Natural Environment Research Council (NERC) and  
350 the German Federal Ministry of Education and Research(BMBF). The ROV work was supported  
351 by the Helmholtz Infrastructure Initiative “Frontiers in Arctic marine Monitoring” (FRAM). We  
352 are thankful to the captain, crew and scientists onboard the *IB Oden*, as well as to the SPRS and  
353 AWI logistics for facilitating our participation in the AO18 expedition. Our special thanks go to  
354 Matthieu Labaste, Helen Czerski and Lars Lehnert for their field support, Ruzica Dadic for her  
355 advice on snow, and the polar bear guarding crew for keeping us safe.

356

### 357 **Data availability**

358 All data presented in this study are publicly available under the following DOIs:

359 ROV: <https://doi.org/10.1594/PANGAEA.925698>

360 Magna Probe and GEM2: <https://doi.pangaea.de/10.1594/PANGAEA.934431>

361 Aerial images: <https://doi.org/10.5281/zenodo.5119094>

362

### 363 **Competing interest**

364 The authors declare that they have no conflict of interest.

365

### 366 **References**

- 367 Ardyna, M., Mundy, C. J., Mills, M. M., Oziel, L., Grondin, L. L., Verin, G., et al. (2020).  
368 Environmental drivers of under-ice phytoplankton bloom dynamics in the Arctic Ocean.  
369 *Elementa: Science of the Anthropocene*, 8(30). doi:10.1525/elementa.430
- 370 Arndt, S., & Nicolaus, M. (2014). Seasonal cycle and long-term trend of solar energy fluxes  
371 through Arctic sea ice. *The Cryosphere*, 8(6). doi:10.5194/tc-8-2219-2014
- 372 Arrigo, K. R. (2014). Sea ice ecosystems. *Annual Review of Marine Science*, 6(1).  
373 doi:10.1146/annurev-marine-010213-135103
- 374 Bintanja, R. (1999). On the glaciological, meteorological, and climatological significance of  
375 Antarctic blue ice areas. *Reviews of Geophysics*, 37(3). doi:10.1029/1999rg900007
- 376 Colbeck, S. C. (1979). Sintering and compaction of snow containing liquid water. *Philosophical  
377 Magazine A*, 39(1). doi:10.1080/01418617908239272
- 378 Dadic, R., Mott, R., Horgan, H. J., & Lehning, M. (2013). Observations, theory, and modeling of  
379 the differential accumulation of Antarctic megadunes. *Journal of Geophysical Research:  
380 Earth Surface*, 118(4). doi:10.1002/2013jf002844
- 381 Edström, P. (2005). A Fast and Stable Solution Method for the Radiative Transfer Problem. *SIAM  
382 Rev.*, 47(3). doi:10.1137/s0036144503438718
- 383 Ehn, J. K., Papakyriakou, T. N., & Barber, D. G. (2008). Inference of optical properties from  
384 radiation profiles within melting landfast sea ice. *Journal of Geophysical Research*,  
385 113(C09024). doi:10.1029/2007jc004656
- 386 Ehn, J. K., Mundy, C. J., Barber, D. G., Hop, H., Rossnagel, A., & Stewart, J. (2011). Impact of  
387 horizontal spreading on light propagation in melt pond covered seasonal sea ice in the  
388 Canadian Arctic. *Journal of Geophysical Research*, 116. doi:10.1029/2010jc006908
- 389 Fetterer, F., & Untersteiner, N. (1998). Observations of melt ponds on Arctic sea ice. *Journal of  
390 Geophysical Research: Oceans*, 103(C11). doi:10.1029/98jc02034
- 391 Frezzotti, M., Gandolfi, S., & Urbini, S. (2002a). Snow megadunes in Antarctica: Sedimentary  
392 structure and genesis. *Journal of Geophysical Research*, 107(D18).  
393 doi:10.1029/2001jd000673
- 394 Frezzotti, M., Gandolfi, S., La Marca, F., & Urbini, S. (2002b). Snow dunes and glazed surfaces  
395 in Antarctica: new field and remote-sensing data. *Annals of Glaciology*, 34.  
396 doi:10.3189/172756402781817851
- 397 Flocco, D., Feltham, D. L., Bailey, E., & Schroeder, D. (2015). The refreezing of melt ponds on  
398 Arctic sea ice. *Journal of Geophysical Research: Oceans*, 120(2).  
399 doi:10.1002/2014jc010140

- 400 Grenfell, T. C., & Maykut, G. A. (1977). The optical properties of ice and snow in the Arctic  
401 Basin. *Journal of Glaciology*, 18(80). doi:10.3189/S0022143000021122
- 402 Hanson, A. (1965). Studies of the Mass Budget of Arctic Pack-Ice Floes. *Journal of Glaciology*,  
403 5(41). doi:10.3189/S0022143000018694
- 404 Hunkeler, P. A., Hoppmann, M., Hendricks, S., Kalscheuer, T., & Gerdes, R. (2016). A glimpse  
405 beneath Antarctic sea ice: Platelet layer volume from multifrequency electromagnetic  
406 induction sounding. *Geophysical Research Letters*, 43(1). doi:10.1002/2015gl065074
- 407 Katlein, C., Arndt, S., Nicolaus, M., Perovich, D. K., Jakuba, M. V., Suman, S., et al. (2015).  
408 Influence of ice thickness and surface properties on light transmission through Arctic sea  
409 ice. *Journal of Geophysical Research: Oceans*, 120(9). doi:10.1002/2015JC010914
- 410 Katlein, C., Schiller, M., Belter, H. J., Coppolaro, V., Wenslandt, D., & Nicolaus, M. (2017). A  
411 New Remotely Operated Sensor Platform for Interdisciplinary Observations under Sea Ice.  
412 *Frontiers in Marine Science*, 4. doi:10.3389/fmars.2017.00281
- 413 Katlein, C., Arndt, S., Belter, H. J., Castellani, G., & Nicolaus, M. (2019). Seasonal Evolution of  
414 Light Transmission Distributions Through Arctic Sea Ice. *Journal of Geophysical  
415 Research: Oceans*, 124(8). doi:10.1029/2018jc014833
- 416 Katlein, C., Valcic, L., Lambert-Girard, S., & Hoppmann, M. (2021). New insights into radiative  
417 transfer within sea ice derived from autonomous optical propagation measurements. *The  
418 Cryosphere*, 15(1). doi:10.5194/tc-15-183-2021
- 419 Lange, B. A., Flores, H., Michel, C., Beckers, J. F., Bublit, A., Casey, J. A., et al. (2017). Pan-  
420 Arctic sea ice-algal chl a biomass and suitable habitat are largely underestimated for  
421 multiyear ice. *Global Change Biology*, 23(11). doi:10.1111/gcb.13742
- 422 Lee, S. H., McRoy, C. P., Joo, H. M., Gradinger, R., Cui, H., Yun, M. S., et al. (2011). Holes in  
423 Progressively Thinning Arctic Sea Ice Lead to New Ice Algae Habitat. *Oceanography*,  
424 24(3). doi:10.5670/oceanog.2011.81
- 425 Light, B., Grenfell, T. C., & Perovich, D. K. (2008). Transmission and absorption of solar radiation  
426 by Arctic sea ice during the melt season. *Journal of Geophysical Research*, 113(C03023).  
427 doi:10.1029/2006jc003977
- 428 Light, B., Perovich, D. K., Webster, M. A., Polashenski, C., & Dadic, R. (2015). Optical properties  
429 of melting first-year Arctic sea ice. *Journal of Geophysical Research: Oceans*, 120(11).  
430 doi:10.1002/2015jc011163
- 431 Lu, P., Cao, X., Wang, Q., Leppäranta, M., Cheng, B., & Li, Z. (2018). Impact of a Surface Ice  
432 Lid on the Optical Properties of Melt Ponds. *Journal of Geophysical Research: Oceans*,  
433 123(11). doi:10.1029/2018jc014161
- 434 Massom, R. A., Drinkwater, M. R., & Haas, C. (1997). Winter snow cover on sea ice in the  
435 Weddell Sea. *Journal of Geophysical Research: Oceans*, 102(C1). doi:10.1029/96jc02992
- 436 Maykut, G. A. (1978). Energy exchange over young sea ice in the central Arctic. *Journal of  
437 Geophysical Research*, 83(C7). doi:10.1029/JC083iC07p03646
- 438 Merkouriadi, I., Cheng, B., Graham, R. M., Rösel, A., & Granskog, M. A. (2017). Critical Role of  
439 Snow on Sea Ice Growth in the Atlantic Sector of the Arctic Ocean. *Geophysical Research  
440 Letters*, 44(20). doi:10.1002/2017gl075494
- 441 Nicolaus, M., Katlein, C., Maslanik, J., & Hendricks, S. (2012). Changes in Arctic sea ice result  
442 in increasing light transmittance and absorption. *Geophysical Research Letters*, 39(24).  
443 doi:10.1029/2012gl053738

- 444 Perovich, D. K. (1990). Theoretical estimates of light reflection and transmission by spatially  
445 complex and temporally varying sea ice covers. *Journal of Geophysical Research*, *95*(C6).  
446 doi:10.1029/JC095iC06p09557
- 447 Perovich, D. K., Tucker III, W. B., & Ligett, K. A. (2002). Aerial observations of the evolution of  
448 ice surface conditions during summer. *Journal of Geophysical Research*, *107*(C10).  
449 doi:10.1029/2000jc000449
- 450 Perovich, D. K., Grenfell, T. C., Richter-Menge, J. A., Light, B., Tucker III, W. B., & Eicken, H.  
451 (2003). Thin and thinner: Sea ice mass balance measurements during SHEBA. *Journal of*  
452 *Geophysical Research*, *108*(C3). doi:10.1029/2001jc001079
- 453 Perovich, D. K., Grenfell, T. C., Light, B., Elder, B. C., Harbeck, J. P., Polashenski, C., et al.  
454 (2009). Transpolar observations of the morphological properties of Arctic sea ice. *Journal*  
455 *of Geophysical Research*, *114*(C00A04). doi:10.1029/2008jc004892
- 456 Perovich, D. K., Richter-Menge, J. A., Jones, K. F., Light, B., Elder, B. C., Polashenski, C., et al.  
457 (2011). Arctic sea-ice melt in 2008 and the role of solar heating. *Annals of Glaciology*,  
458 *52*(57). doi:10.3189/172756411795931714
- 459 Perron, C., Katlein, C., Lambert-Girard, S., Leymarie, E., Guinard, L.-P., Marquet, P., et al. (2021).  
460 Development of a Diffuse Reflectance Probe for In Situ Measurement of Inherent Optical  
461 Properties in Sea Ice, *The Cryosphere Discuss.*, in review, doi:10.5194/tc-2021-104
- 462 Petrich, C., Eicken, H., Polashenski, C. M., Sturm, M., Harbeck, J. P., Perovich, D. K., et al.  
463 (2012a). Snow dunes: A controlling factor of melt pond distribution on Arctic sea ice.  
464 *Journal of Geophysical Research: Oceans*, *117*(C09029). doi:10.1029/2012jc008192
- 465 Petrich, C., Nicolaus, M., & Gradinger, R. (2012b). Sensitivity of the light field under sea ice to  
466 spatially inhomogeneous optical properties and incident light assessed with three-  
467 dimensional Monte Carlo radiative transfer simulations. *Cold Regions Science and*  
468 *Technology*, *73*. doi:10.1016/j.coldregions.2011.12.004
- 469 Polashenski, C., Perovich, D. K., & Courville, Z. (2012). The mechanisms of sea ice melt pond  
470 formation and evolution. *Journal of Geophysical Research: Oceans*, *117*(C1).  
471 doi:10.1029/2011jc007231
- 472 Rösel, A., Kaleschke, L., & Birnbaum, G. (2012). Melt ponds on Arctic sea ice determined from  
473 MODIS satellite data using an artificial neural network. *The Cryosphere*, *6*(2).  
474 doi:10.5194/tc-6-431-2012
- 475 Schröder, D., Feltham, D. L., Flocco, D., & Tsamados, M. (2014). September Arctic sea-ice  
476 minimum predicted by spring melt-pond fraction. *Nature Climate Change*, *4*(5).  
477 doi:10.1038/nclimate2203
- 478 Sturm, M., Holmgren, J., König, M., & Morris, K. (1997). The thermal conductivity seasonal  
479 snow. *Journal of Glaciology*, *43*(143). doi:10.3189/S0022143000002781
- 480 Sturm, M., Holmgren, J., & Perovich, D. K. (2002). Winter snow cover on the sea ice of the Arctic  
481 Ocean at the Surface Heat Budget of the Arctic Ocean (SHEBA): Temporal evolution and  
482 spatial variability. *Journal of Geophysical Research*, *107*(C10).  
483 doi:10.1029/2000jc000400
- 484 Sturm, M., & Holmgren, J. (2018). An Automatic Snow Depth Probe for Field Validation  
485 Campaigns. *Water Resources Research*, *54*(11). doi:10.1029/2018wr023559
- 486 Untersteiner, N. (1961). On the Mass and Heat Budget of Arctic Sea Ice. *Archiv für Meteorologie,*  
487 *Geophysik und Bioklimatologie, Serie A*, *12*. doi:10.1007/BF02247491

- 488 Van den Broeke, M., & Bintanja, R. (1995). Summertime Atmospheric Circulation in the Vicinity  
489 of a Blue Ice Area in Queen Maud Land, Antarctica. *Boundary-Layer Meteorology*, 72(4).  
490 doi:10.1007/BF00709002
- 491 Vüllers, J., Achtert, P., Brooks, I. M., Tjernström, M., Prytherch, J., Burzik, A., et al. (2021).  
492 Meteorological and cloud conditions during the Arctic Ocean 2018 expedition.  
493 *Atmospheric Chemistry and Physics*, 21(1). doi:10.5194/acp-21-289-2021
- 494 Webster, M. A., Rigor, I. G., Nghiem, S. V., Kurtz, N. T., Farrell, S. L., Perovich, D. K., et al.  
495 (2014). Interdecadal changes in snow depth on Arctic sea ice. *Journal of Geophysical*  
496 *Research: Oceans*, 119(8). doi:10.1002/2014jc009985
- 497 Webster, M. A., Rigor, I. G., Perovich, D. K., Richter-Menge, J. A., Polashenski, C. M., & Light,  
498 B. (2015). Seasonal evolution of melt ponds on Arctic sea ice. *Journal of Geophysical*  
499 *Research: Oceans*, 120(9). doi:10.1002/2015jc011030
- 500 Webster, M. A., Gerland, S., Holland, M. M., Hunke, E., Kwok, R., Lecomte, O., et al. (2018).  
501 Snow in the changing sea-ice systems. *Nature Climate Change*, 8(11).  
502 doi:10.1038/s41558-018-0286-7  
503